THE ASTROPHYSICAL JOURNAL, 504:1029–1034, 1998 September 10

ACOUSTIC POWER MAPS OF SOLAR ACTIVE REGIONS

BRADLEY W. HINDMAN
JILA, University of Colorado, Boulder CO 80309; hindman@hao.ucar.edu

AND

TIMOTHY M. BROWN
High Altitude Observatory, National Center for Atmospheric Research, P.O. Box 3000, Boulder, CO 80307-3000
Received 1998 March 2; accepted 1998 April 14

ABSTRACT

Using observations made by the Michelson Doppler Imager (MDI), we find that within solar active regions the spatial distributions of Doppler velocity power and continuum intensity power differ. The oscillation power within any pixel is a strong function of the magnetic field strength within that pixel. The amplitudes of oscillations with frequencies less than 5.2 mHz decrease with field strength for both velocity and continuum intensity measurements. However, within active regions oscillations with frequencies between 5.2 and 7.0 mHz have suppressed continuum intensity amplitudes but enhanced velocity amplitudes. The enhancement of the high-frequency velocity signal is largest in pixels with intermediate field strength (50–250 G) and is a manifestation of the high-frequency acoustic halos. We find that the high-frequency halos are absent in MDI observations of the continuum intensity.

Subject headings: Sun: magnetic fields — Sun: oscillations — Sun: photosphere

1. INTRODUCTION

The frequencies of solar eigenmodes (*p*-modes) have been used extensively over the last two decades to determine the properties of the cavity within which the oscillations are trapped. Such techniques, however, have not successfully measured the properties of the solar magnetic field. Deep within the convection zone the Sun's magnetic field is too weak to produce a significant modification of the eigenfrequencies. Only in the surface layers does the magnetic field become dynamically significant. However, the effect of the magnetic field in the surface layers is difficult to extract from frequency measurements because of many nonmagnetic surface effects which compete in shifting mode frequencies.

The frequencies are not the only source of information provided by the solar oscillations. Measurements of the surface amplitude of the oscillations can also be used as a seismic probe. The surface amplitude can be strongly modified by the presence of a magnetic field. It has been known since the origination of helioseismology that the amplitudes of *p*-modes are reduced in regions with a magnetic field (Leighton, Noyes, & Simon 1962; Lites, White, & Packman 1982; Tarbell et al. 1988; Title et al. 1992). More recently, it has been discovered that the amplitudes of untrapped high-frequency oscillations can be increased by the presence of a magnetic field. Using Ca II K-line images, Braun et al. (1992) observed that oscillations with frequencies between 5.5 and 6.5 mHz have an enhanced signal in rings surrounding regions of intense field strength. With Doppler velocity measurements taken with the Fe I λ5576 line, similar results were found by Brown et al. (1992), except that the rings were patchier and were confined to the edges of the active region instead of extending into the surrounding quiet Sun. This region of excess high-frequency oscillation power has been dubbed a halo, and both studies have interpreted the halos as regions of enhanced acoustic emission.

The intent of this study is to measure and quantify the surface amplitudes in regions of quiet Sun and in active regions in order that the mechanisms responsible for the observed amplitude changes can be deduced. The conjecture that the acoustic emissivity or scattering is modified by the presence of a magnetic field is extremely plausible, but it is not the only conceivable explanation. Cally (1995) has suggested that the reduction in *p*-mode amplitude within active regions is caused by the absorption of acoustic waves by magnetic structures (Braun, Duvall, & LaBonte 1988; Bogdan et al. 1993). Alternatively, the energy present in the acoustic oscillations may be unchanged, but the value of the acoustic wave functions within the surface layers may be altered (Hindman, Jain, & Zweibel 1997), or the acoustic motions may become field aligned, increasing the observed line-of-sight velocity component. Finally, purely observational effects may change the measured surface amplitude as well. The presence of a magnetic field can modify the thermal structure of the atmosphere, thereby altering the height of formation of the spectral lines used to measure the oscillations. Since the acoustic wave functions are functions of height, the measured surface amplitudes change as a consequence.

All of these mechanisms should have distinctive dependences on wave frequency and magnetic field strength. Therefore, in order to differentiate between the various possibilities, careful analysis of the surface amplitude as a function of these quantities is crucial. In this paper we perform such an analysis using Michelson Doppler Imager (MDI) observations of the Doppler velocity, continuum intensity, and line-of-sight magnetic field strength.

2. THE OBSERVATIONS

In normal operating mode the MDI instrument (Scherrer et al. 1995) produces five filtergram images centered at equally spaced wavelengths across the Ni I λ6768 spectral line. By taking these five filtergram measurements in different combinations, the Doppler velocity, continuum intensity, and line depth are obtained. In addition, by subtracting the Doppler shifts calculated separately in right- and left-handed circularly polarized light, the line-of-sight magnetic field strength can be measured using the Zeeman effect.

MDI measures the continuum intensity in two ways: a single filtergram in a clean portion of the solar spectrum far removed from line center can be used, or all five filtergrams can be combined. This study utilized single filtergram measurements of the continuum intensity.

The observations used in this study were taken over a duration of 4 hr 26 minutes on 1996 November 21. Using the high-resolution field of view (0″.605 square pixels), MDI made measurements every minute of the line-of-sight velocity, the continuum intensity, and the line-of-sight magnetic field strength. During the time the observations were made, the high-resolution field of view contained a small dipolar active region. We analyzed a 193″.7 square subfield that contained this active region and a large patch of quiet Sun. The center of this subfield was located 160″.7 from solar center and 102″.5 above the solar equator at the beginning of the observations. The left panel of Figure 1 is a magnetogram of this subfield taken early in the observation run.

From the time series of the magnetic field strength, we calculate the rms field strength for each pixel. The right panel of Figure 1 shows the rms field strength over the entire duration of the observations. At each pixel, the time series of the fluctuating part of the velocity and continuum intensity were Fourier-transformed to produce acoustic power maps of the region at each frequency. The effects of granulation were removed from the velocity and intensity fluctuations by filtering out signals with frequencies less than the *f*-mode in the frequency-wavenumber domain.

3. THE ANALYSIS AND RESULTS

Once the power spectrum at each pixel was computed, we created acoustic power maps by summing the power over two frequency ranges. Figure 2 displays four power maps of the same region shown in the magnetogram of Figure 1. The left panels are power maps created from the Doppler velocity and the right panels are maps created from the continuum intensity fluctuations. The upper panels were constructed by summing power over all frequencies corresponding to trapped *p*-mode oscillations, $\nu < 5.2$ mHz. The lower panels are the results of summation over high-frequency oscillations between 5.5 and 6.5 mHz.

From comparison of the top panels of Figure 2 with the magnetograms of Figure 1, it can easily be seen that the amplitudes of the oscillations below 5.2 mHz are suppressed in regions of strong magnetic field. Both the velocity measurements and the intensity measurements produce similar spatial distributions of power. From the lower panels of Figure 2, it is obvious that the high-frequency oscillations have different power distributions of velocity and continuum intensity. The high-frequency velocity power map shows that the oscillations have enhanced amplitude in the general area of the active region, whereas the high-frequency continuum intensity power is suppressed in an identical fashion as the lower frequency *p*-modes. The power enhancement in the high-frequency velocity map is the same phenomenon as the high-frequency acoustic halos previously discussed by Braun et al. (1992) and Brown et al. (1992). The active region we are investigating has a wispy structure without a well-defined center. Therefore, the power enhancement appears less like a halo and more like a patch overlying the active region. Nevertheless, the halo is completely absent in the continuum intensity data.

The power maps of Figure 2 in conjunction with the magnetograms of Figure 1 indicate that the solar oscillations have surface amplitudes that are strong functions of frequency and magnetic field strength. Figures 3 and 4 show the results of more detailed investigation of the dependences of the oscillation power on these factors. Figure 3 consists of five panels, each corresponding to the range of rms field strengths indicated at the top of the panel. In addition, the average rms field strength of all pixels falling within the range is shown. Each panel displays the average power of

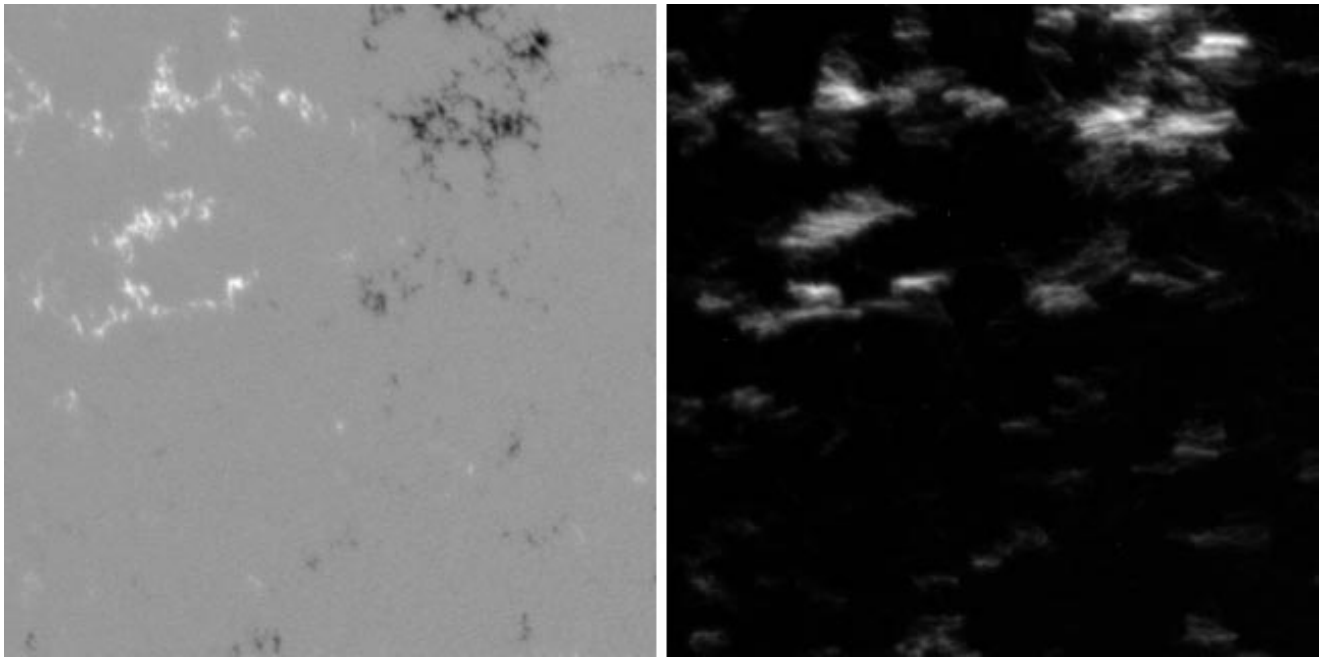

FIG. 1.—*Left*: Magnetogram of the region used in the analysis taken early in the set of observations. The maximum field strength is 1816 G. *Right*: Image of the rms field strength of the entire set of observations.

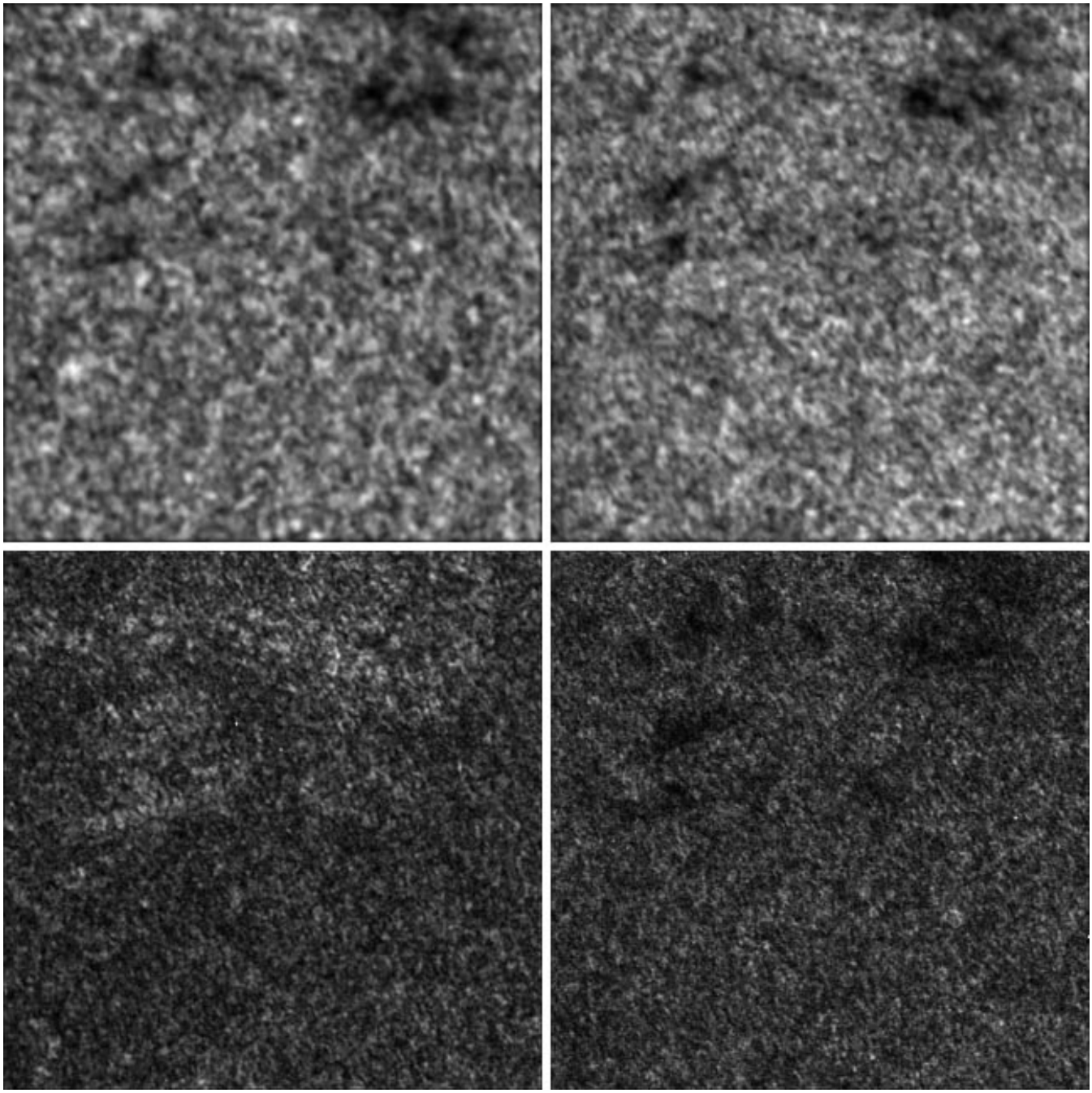

FIG. 2.—*Left*: Power maps made from the Doppler velocity. *Right*: Maps made from the continuum intensity fluctuations. The upper panels were constructed by summing over all frequencies corresponding to *p*-modes, $\nu < 5.2$ mHz. The lower panels are the results of summation over high-frequency oscillations between 5.5 and 6.5 mHz.

pixels within the appropriate field strength range as a function of frequency normalized by the same result for the quiet Sun. Quiet pixels were defined as any pixel with an rms field strength of less than 10 G. In each panel the solid line is the result for the Doppler velocity measurements and the dashed line is for continuum intensity measurements. A power ratio of 1 indicates that the power in magnetized pixels is consistent with the power in the quiet Sun. We do not show results for frequencies less than 1.5 mHz because the oscillation signal is dominated by solar convection at these low frequencies.

The effect of the magnetic field on oscillation power becomes important at fairly low field strengths. The difference in power between magnetized pixels and quiet pixels becomes evident for field strengths greater than 20 G. Considering that MDIs per pixel measurement uncertainty is roughly 20 G, the magnetic field could be important for even lower field strengths, but the observations are unable to distinguish the difference between any fields less than 20 G in strength. As the field strength increases, the power below 5 mHz is suppressed compared to the quiet Sun for both the Doppler velocity measurements and the continuum intensity measurements. The suppression grows with field strength, and at the largest strengths the reduction in power can be as large as 60%. Above 5 mHz the continuum intensity power continues to be suppressed. The Doppler

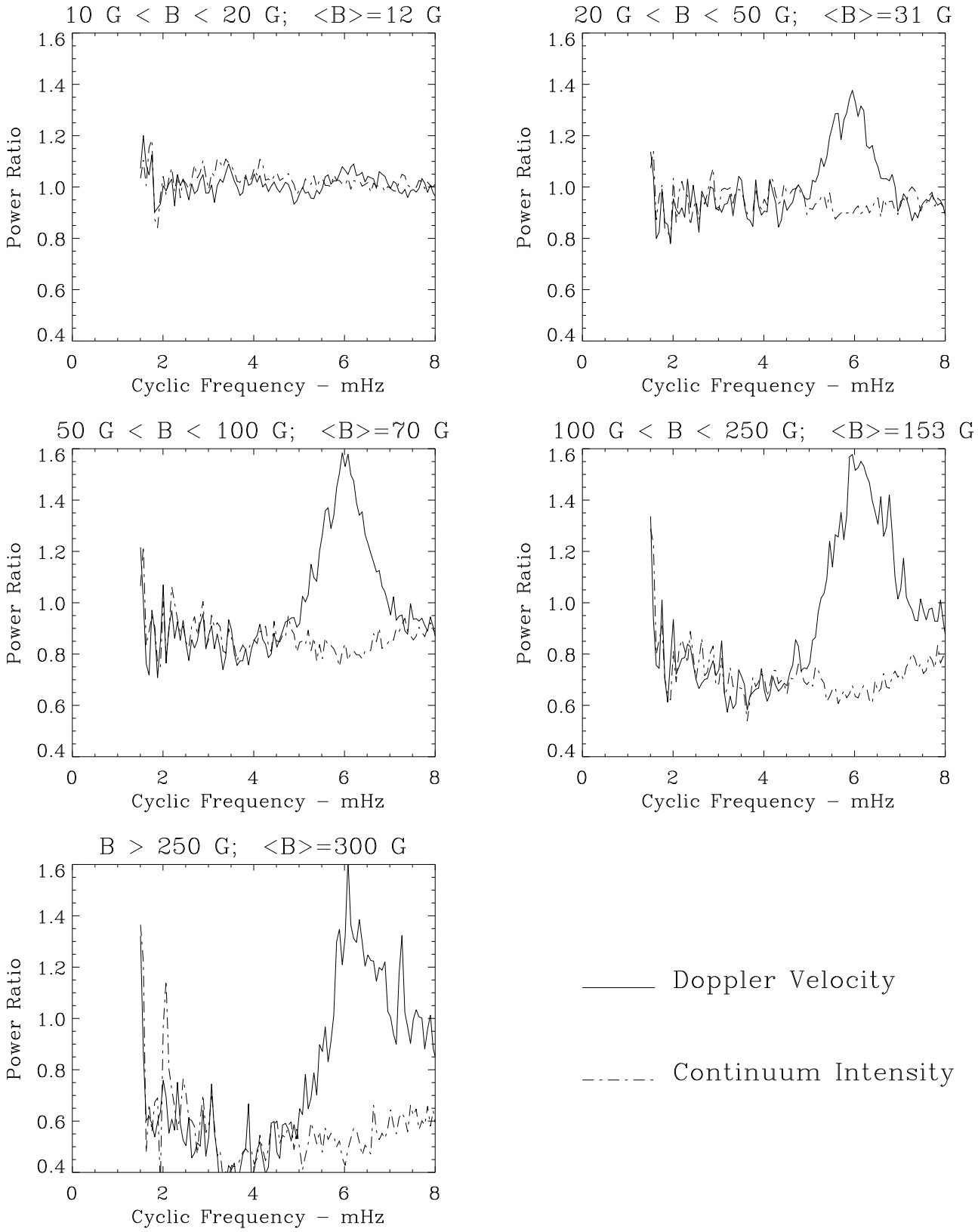

FIG. 3.—Each panel shows the ratio of the power of magnetized pixels over the power of quiet pixels as a function of frequency. For each panel the range of rms magnetic field strengths allowed in the set of magnetized pixels is shown at the top of the panel. In addition, the average rms field strength of this set of pixels is indicated. The solid curve is the result for the Doppler velocity data, and the dashed curve is for the continuum intensity data.

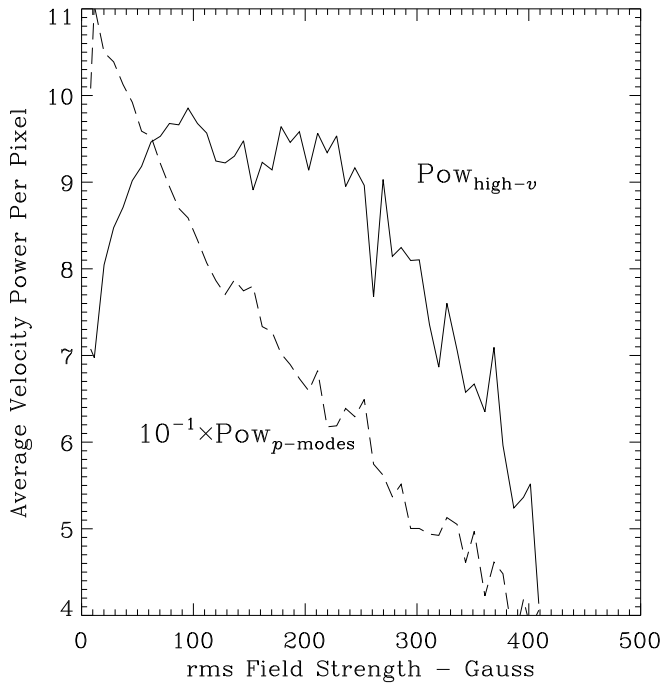

FIG. 4.—Oscillatory power of the velocity for oscillations between 5.5 and 6.5 mHz (*solid line*) and for oscillations lower than 5 mHz (*dashed line*) as a function of magnetic field strength. The dashed curve has been divided by a factor of 10 in order to show both curves on the same graph.

velocity power, however, has a strong power enhancement in magnetized pixels compared to quiet pixels. The enhancement is sharply peaked at 6 mHz, reaching values as large as 60%. This enhancement at 6 mHz is the result of the high-frequency acoustic halo.

A careful study of the panels of Figure 3 suggests that the halos are strongest in pixels with intermediate field strength (50–250 G). Figure 4 displays this property more clearly. In arbitrary units the solid line shows the power within the high-frequency band, 5.5–6.5 mHz, summed over all pixels with like rms magnetic field strength. The dashed curve shows the same quantity for power within the *p*-mode frequency range, $\nu < 5.2$ mHz, scaled by a factor of 10^{-1} in order to display the dashed and solid curves on the same graph. It is clearly seen that the high-frequency power is largest for pixels with field strengths between 50 and 250 G. It is also apparent that the amplitude of high-frequency oscillations is reduced in pixels with the highest field strengths ($B > 350$ G).

4. CONCLUSIONS

It is now well established that the surface amplitudes of solar oscillations are modified by the presence of a magnetic field. This study and many others have shown that the amplitudes of oscillations below 5.2 mHz are reduced in the presence of a magnetic field (Leighton, Noyes, & Simon 1962; Tarbell et al. 1988; Title et al. 1992). Furthermore, Doppler velocity and Ca II K-line intensity observations show that oscillations with frequencies between 5.5 and 6.5 mHz have enhanced amplitudes in halos surrounding active regions. The suppression of *p*-mode amplitudes and the presence of high-frequency halos are also observed in MDI measurements of the Ni 6768 Å line depth fluctuations (Jain & Haber 1998).

Using MDI observations, we find that the suppression of *p*-mode amplitudes within magnetized regions of the Sun has a frequency dependence. The suppression increases with frequency until a broad minimum in reduced power is achieved around 4 mHz. For frequencies less than 5 mHz the velocity and continuum intensity data have identical suppression factors. Above 5 mHz the continuum intensity continues to be suppressed in pixels with a magnetic field, while the velocity has an enhancement sharply peaked at 6 mHz. Correspondingly, the intensity power maps lack the high-frequency halos that are seen in velocity power maps. A careful examination of the high-frequency power shows that the halos observed by MDI are largely confined to pixels with intermediate field strength (50–250 G).

The interpretation of Braun et al. (1992) and Brown et al. (1992) that the high-frequency halos are regions with increased acoustic emissivity or scattering is not supported by our finding that the halos are absent in continuum intensity power maps. If the enhanced power of the halos is produced by increased generation of acoustic waves, the temperature perturbations induced by these compressive oscillations should result in observed intensity fluctuations as well as a Doppler velocity signal. The high-frequency halos were initially observed by Braun et al. (1992) using Ca II K-line intensity observations. This apparent inconsistency with the absence of halos in the MDI intensity observations has a possible explanation. The Ca II K-line intensity measurements were made using a broad filter that spanned both the wings and the core of the spectral line. Such a measurement is susceptible to contamination from Doppler shifts that move the spectral line back and forth across the filter, producing variations in the observed intensity. Therefore, the observations of Braun et al. (1992) are incapable of distinguishing true intensity variations from velocity perturbations.

Another possible interpretation is that the magnetic field, which is primarily vertical at the photosphere, ducts the acoustic oscillations into field-aligned motions. Therefore, observations at disk center would register an increased line-of-sight velocity signal without a corresponding increase in continuum intensity signal. A simple check of this hypothesis can be accomplished by observing the acoustic halos on different portions of the solar disk. Observations made near the solar limb would have negligible amplitude enhancement, and the center-to-limb variation should have a predictable geometric dependence. Although this test has not yet been performed explicitly, the Ca II K-line observations of Toner & LaBonte (1993) span the entire solar disk, and their high-frequency acoustic power maps do not reveal any obvious latitudinal variation in halo power. However, it must be kept in mind that the analysis of Toner & LaBonte (1993) is not ideal for addressing this question. They average their power maps over 7 days of data. Over this period a given Carrington longitude has rotated a significant amount, thereby destroying any center-to-limb variation that might be seen as a function of longitude.

The fact that the halos are absent in observations of the continuum intensity suggests that the halos are produced by incompressible oscillations, such as Alfvén waves or transverse magnetic flux tube waves (kink waves). Perhaps the magnetic waves are generated on field lines at the boundary of active regions. Vigorous convection in the quiet Sun surrounding the active region could buffet boundary field lines exciting magnetic oscillations, or perhaps

acoustic waves propagating in from the quiet Sun shake the magnetic flux tubes in the boundary, creating magnetic waves. If the field lines above the active region expand into a magnetic canopy in the chromosphere, the ring of enhanced power should expand with height, because the magnetic oscillations will propagate along the magnetic field lines. Indeed, this is what is seen. Observations of the halos using Fe I λ5576 or Ni I λ6768, which are formed in the photosphere and temperature minimum, show compact halos that are confined to the edges of active regions. Observations using Ca II K, however, have larger halos, which extend into the surrounding quiet Sun. The Ca II K line is formed higher in the atmosphere than the Fe I or Ni I lines. A more detailed examination of the height dependence of the halos is being performed by D. Stanchfield and J. H. Thomas (1997, private communication). They are examining observations of an active regions with simultaneous measurement using Ca II K and the High Altitude Observatory's Advanced Stokes Polarimeter.

We are indebted to Tom Bogdan, Colin Rosenthal, and Ellen Zweibel for useful discussions concerning the implication of this work. We thank the SOI/MDI team for making their web page such a simple way to obtain MDI data. We gratefully acknowledge the financial support of the Advanced Studies Program and the High Altitude Observatory, divisions of the National Center for Atmospheric Research. The National Center for Atmospheric Research is sponsored by the National Science Foundation.

REFERENCES

Bogdan, T. J., Brown, T. M., Lites, B. W., & Thomas, J. H. 1993, ApJ, 406, 723
Braun, D. C., Duvall, T. L., Jr., & LaBonte, B. J. 1988, ApJ, 335, 1015
Braun, D. C., Lindsey, C., Fan, Y., & Jefferies, S. M. 1992, ApJ, 392, 739
Brown, T. M, Bogdan, T. J., Lites, B. W., & Thomas, J. H. 1992, ApJ, 394, L65
Cally, P. S. 1995, ApJ, 451, 372
Hindman, B. W., Jain, R., & Zweibel, E. G. 1997, ApJ, 476, 392
Haber, D., & Jain, R. 1998, in preparation
Leighton, R. B., Noyes, R. W., & Simon, G. W. 1962, ApJ, 135, 474
Lites, B. W., White, O. R., & Packman, D. 1982, ApJ, 253, 386
Scherrer, P. H., et al. 1995, Sol. Phys., 162, 129
Tarbell, T. D., Peri, M., Frank, Z., Shine, R., & Title, A. 1988, in Seismology of the Sun and Sun-like Stars, ed. V. Domingo & E. J. Rolfe (SP-286; Noordwijk: ESA), 315
Title, A. M., Topka, K. P., Tarbell, T. D., Schmidt, W., Balke, C., Scharmer, G. 1992, ApJ, 393, 782
Toner, C. G., & LaBonte, B. J. 1993, ApJ, 415, 847